

# BALLISTIC IMPACT OF STRUCTURAL CERAMICS AT HIGH TEMPERATURES

Hideaki Kasano and Osamu Hasegawa

Department of Mechanical Systems Engineerin, Takushoku University  
815-1 Tatemachi, Hachioji City, Tokyo 193-0985, Japan  
hkasano@ms.takushoku-u.ac.jp

## ABSTRACT

Ballistic impact tests are performed using a steel ball projectile on four kinds of monolithic ceramics of  $\text{Al}_2\text{O}_3$ ,  $\text{Si}_3\text{N}_4$ ,  $\text{SiC}$ , and  $\text{ZrO}_2$  at high temperatures of 1000 °C and 1350 °C. For this purpose, an impact test system is developed, which comprises a gas gun type impact machine, a high temperature furnace, and a digital imaging system. The projectile's motion and impact response of these target materials during testing are visualized simultaneously through the digital imaging system. The semi-empirical expressions proposed in our previous paper is applied for estimating/predicting the ballistic impact properties of these materials. The residual velocity and energy absorption ratio are graphically presented as a function of impact velocity for the cases of three different temperatures including a room temperature, which are compared to each other.

## 1. INTRODUCTION

Ceramic materials have attracted great interest for structural applications requiring superior performance at high temperatures because of their high stiffness, low density, and high heat-resistance. One of the potential applications of these materials is advanced gas turbine engine components such as combustion liners, turbine blades, and discs. However, monolithic ceramic materials are susceptible to impact loadings due to their brittleness [1], [2], and therefore the application is severely limited. One approach toward reducing the brittleness and enhancing the impact toughness is by incorporating reinforcements such as fibers and particles into ceramic matrix [3]. Some continuous fiber reinforced ceramic matrix composites such as  $\text{Si}_3\text{N}_4/\text{Si}_3\text{N}_4$  and  $\text{SiC}/\text{SiC}$  are currently being developed [4], which are potential candidates for future application to turbine blades and discs. In order to develop new ceramic matrix composites, better understanding of the material properties of reinforcements and matrix materials is required. In particular, ballistic impact properties are critical in the design of ceramic turbine blades since they are threatened by foreign objects like unburned carbon particles travelling at high speed [5]. The present study is aiming at evaluating the ballistic impact properties of monolithic ceramic materials at high temperatures, which are promising matrix materials of future ceramic matrix composites. The ultra-high speed photographs of a projectile perforating a target plate and impact response of the plate are shown in the form of four consecutive pictures, and also the test results are graphically presented.

## 2. HIGH-TEMPERATURE IMPACT TEST SYSTEM

An impact test system is developed by incorporating a high temperature furnace and a digital imaging system with a gas gun type impact machine, which is shown in Fig.1. The impact machine is capable of firing a steel ball projectile of 5mm in diameter and 0.51g by weight at a maximum velocity of 330 m/s by releasing high-pressurized nitrogen gas. The high temperature furnace has a maximum heating capacity of 1500°C

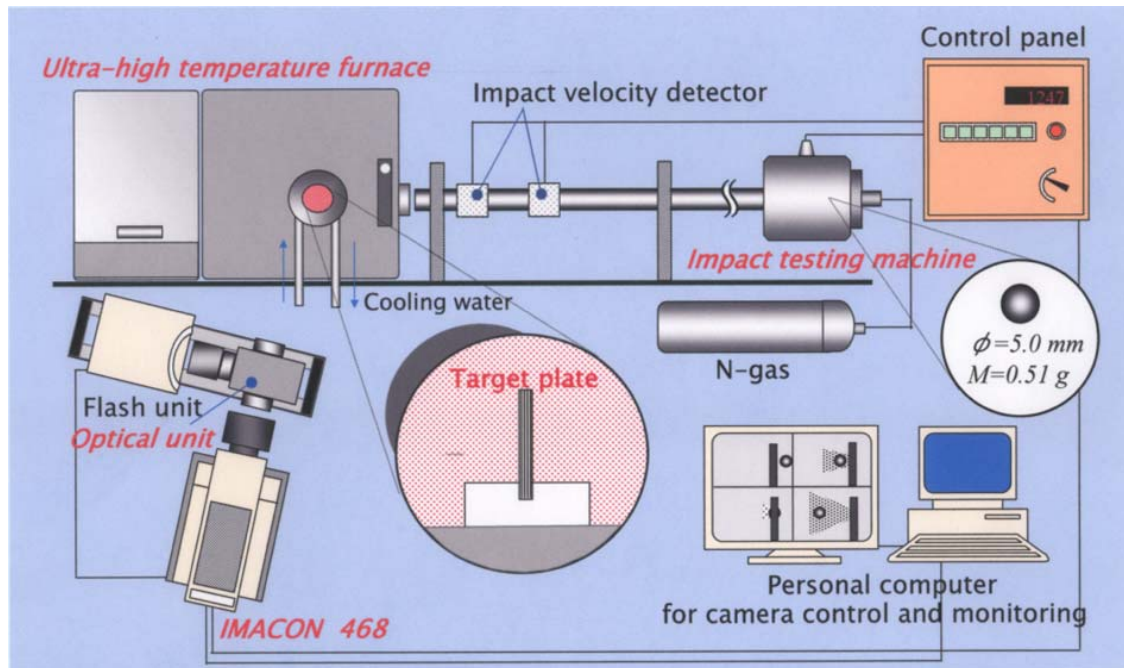


Figure 1: High temperature impact test system

and it has two holes on the two opposite sides, through which the projectile enters and exits from the furnace. The digital imaging system (IMACON 468) consists of an ultra-high speed camera unit, a high-resolution monitor, and a personal computer. The ultra-high speed camera produces four consecutive images, which are displayed on the high-resolution monitor and/or stored in the personal computer for data analysis and image processing.

### 3. TARGET MATERIALS AND BALLISTIC IMPACT TEST

#### 3.1 Target Materials

Target materials investigated in the present study are four kinds of monolithic ceramics of  $\text{Al}_2\text{O}_3$ ,  $\text{Si}_3\text{N}_4$ ,  $\text{SiC}$ , and  $\text{ZrO}_2$ , which are promising matrix materials to be adopted in future ceramic matrix composites. The geometry of the test specimens is a rectangular plate of  $80\text{mm} \times 50\text{mm}$  with thickness of  $1.5\text{mm}$ . The target plate is mounted in the fixture with the lower edge clamped and the others all free, which is kept in the furnace at a high temperature of  $1000\text{ }^\circ\text{C}$  or  $1350\text{ }^\circ\text{C}$ .

#### 3.2 Ballistic Impact Test

In the ballistic impact tests, a steel ball projectile is launched by releasing high-pressurized nitrogen gas and it is accelerated in a barrel of the impact machine. After it exits from the end of the barrel, the projectile enters the furnace through the hole and strikes normally on the target plate. The ultra-high speed photographs of the projectile perforating the target plate and the impact response of the plate are taken through an observation window on the side of the furnace using the digital imaging system, which are displayed on the high-resolution monitor in the form of four consecutive images. The impact velocity just before impact is determined from the elapsed time of the projectile traveling between two specified points using a laser velocity detector located close to the end of the barrel. In the present study, the impact velocities are varied between about  $100\text{m/s}$  and  $260\text{m/s}$ . The residual velocity of the projectile after perforating the target plate is calculated from its change in location on the two consecutive images.

#### 4. PREDICTIONS OF BALLISTIC IMPACT PROPERTIES

Consider a steel ball projectile striking on and perforating a target plate as shown in Fig.2. Then, the ballistic impact properties of this target plate can be characterized using  $V_R$  and  $V_b$ . The  $V_R$  is a residual velocity that is attained just as the projectile passes through and exits from the target plate, while the  $V_b$  is a ballistic limit velocity and it is the velocity beyond which a specified projectile perforates a specified target plate and below which it will not. We consider here only a normal impact of a steel ball projectile on a target plate ( $\phi = 0$ ), and the projectile is assumed to be rigid. The schema of the perforation process is illustrated in Fig.3, in which  $V_i$  is an impact velocity of the projectile,  $v_R$  an average velocity of the scattering plate-fragments,  $M$  mass of the projectile, and  $m$  total mass of the fragments removed from the plate due to the perforation. In our previous paper [6], the semi-empirical expressions for  $V_R$  and  $V_b$  are presented using the balances of momentum and energy as follows:

$$V_b = \sqrt{V_i^2 - V_R^2 / \alpha^2} \quad (1)$$

$$V_R = \alpha \sqrt{V_i^2 - V_b^2} \quad (2)$$

in which, the mass coefficient  $\alpha$  is given by

$$\alpha = \left( \frac{M}{M + m} \right)^{1/2} \quad \alpha = \frac{M}{M + m} \quad (3)$$

for model **A** and **B**, respectively.

Once some pairs of  $V_i$  and  $V_R$  together with  $\alpha$  are obtained from impact tests, the ballistic limit velocity  $V_b$  is estimated from Eq.(1) and then, by substituting it into Eq.(2), the residual velocity  $V_R$  is predicted as a function of impact velocity  $V_i$ .

Perforation energy  $E_p$  and energy absorption ratio  $E_{ab}$  also characterize the ballistic impact properties of the plate, which are defined by

$$E_p = \frac{1}{2} M V_i^2 - \frac{1}{2} M V_R^2 \quad (4)$$

$$E_{ab} = \left( \frac{1}{2} M V_i^2 - \frac{1}{2} M V_R^2 \right) / \frac{1}{2} M V_i^2 \times 100(\%) \quad (5)$$

#### 5. RESULTS AND DISCUSSIONS

The ultra-high speed photographs of the ballistic impact behavior of the target plates and the motion of the steel ball projectile are shown here in the four consecutive images, in which the exposure time is  $2 \mu s$  for all images and the inter-frame time is varied

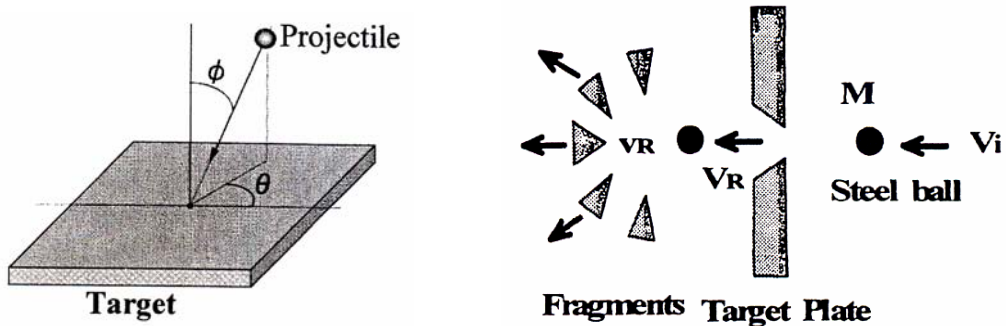


Figure 2: Impact of target plate by a projectile Figure 3: Schema of impact perforation

between 40 and 150  $\mu$  s. The ballistic impact properties of residual velocities of the projectile after perforating the target plate and the energy absorption ratios are also presented graphically as a function of impact velocities for the cases of 1000 °C and 1350 °C along with 23 °C (room temperature) [7]. From the close examination of these photographs and figures, the effect of high temperatures on the ballistic impact behavior and properties of these ceramic materials is investigated.

### 5.1 High-speed Photographs of Ballistic Impact Behavior

Figures 4-7 show examples of the ultra-high speed photographs of the ballistic impact behavior of the target plates of Al<sub>2</sub>O<sub>3</sub>, Si<sub>3</sub>N<sub>4</sub>, SiC and ZrO<sub>2</sub> tested at three different temperatures. From these photos, we find that the target plates are fractured in fragments. For room temperature 23 °C (top), the plate-fragments are mixed with large and small pieces, while, for high temperatures (middle:1000 °C, bottom:1350 °C) they tend to form a cloud of very small pieces, with which the steel ball projectile is covered. We also find that the scattering velocities of the fragments depend on their size and, in general, smaller fragments run ahead of the projectile, which are followed by larger ones. The residual velocities of the projectiles after perforating the target plates are calculated from their change in location using the two consecutive images.

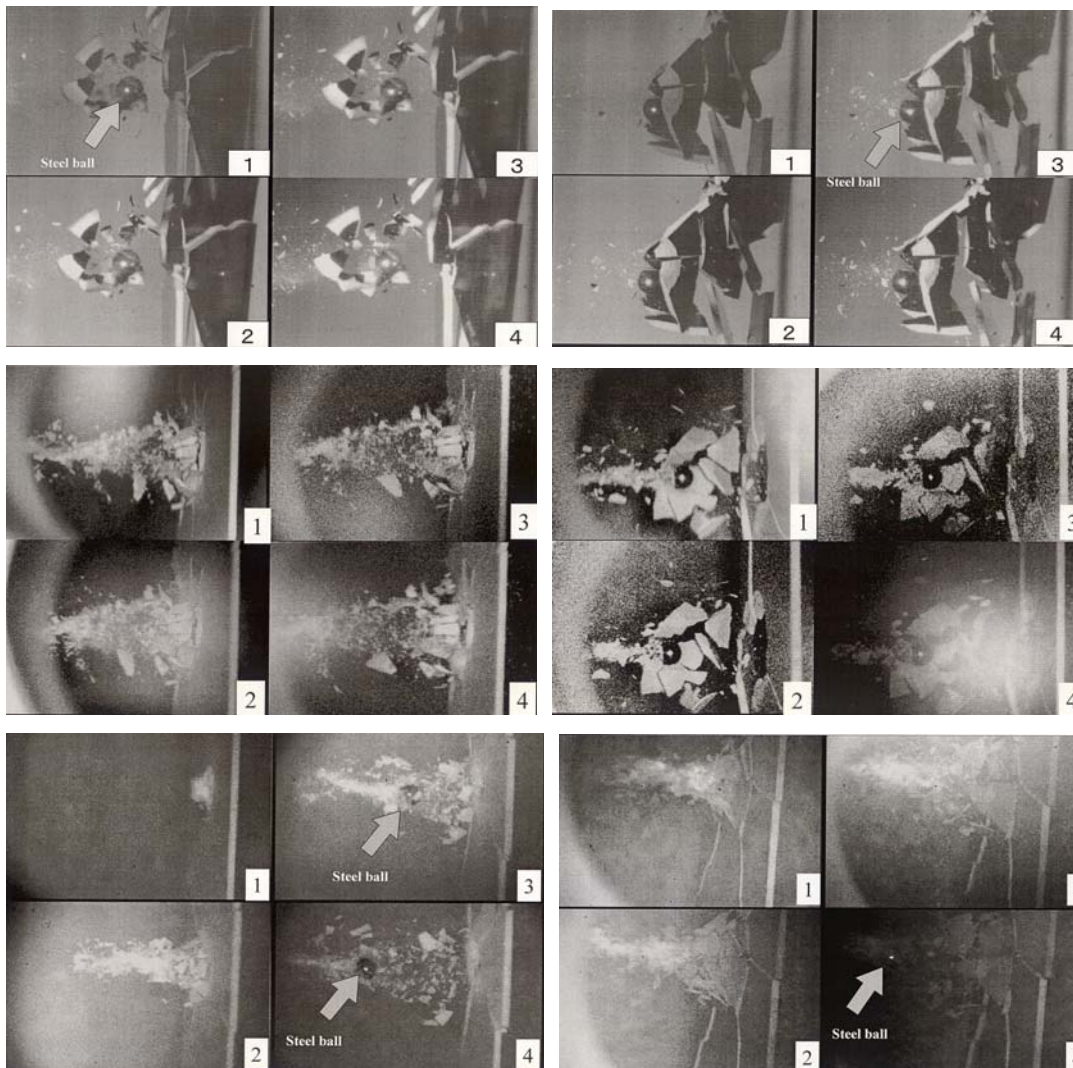


Figure 4: Alumina (Al<sub>2</sub>O<sub>3</sub>)

Figure 5: Silicon Nitride (Si<sub>3</sub>N<sub>4</sub>)

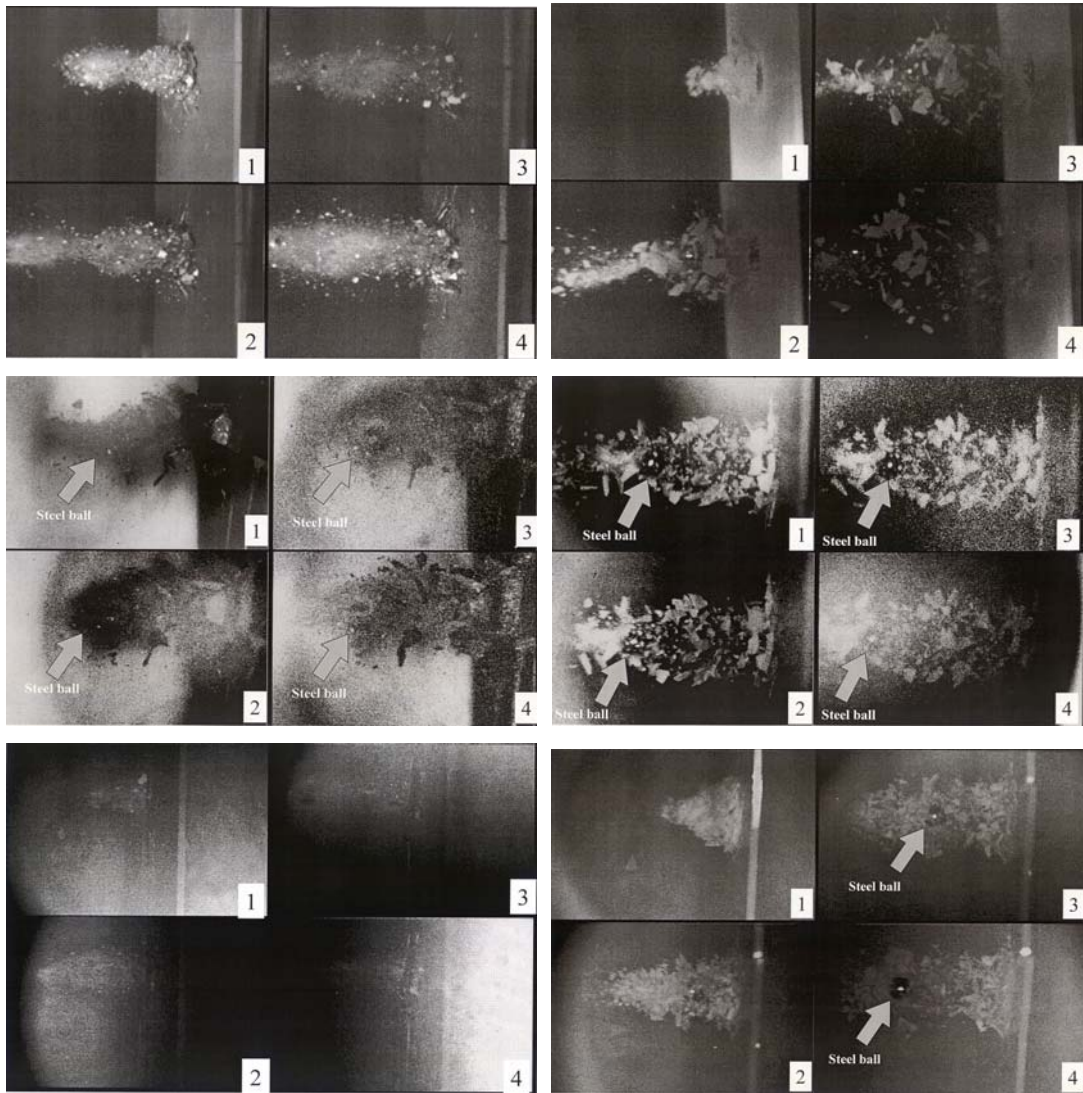


Figure 6: Silicon Carbide (SiC)

Figure 7: Zirconia (ZrO<sub>2</sub>)

The scattering velocities of the fragments, if they can be traced, will also be calculated in a like manner. In the present cases, the impact velocities range from 100 to 180 m/s.

## 5.2 Ballistic Impact Properties

Figure 8 shows the residual velocity  $V_R$  as a function of impact velocity  $V_i$  for SiC and ZrO<sub>2</sub>, in which the results for the case of room temperature 23 °C [7] are also included. In both cases, with an increasing impact velocity, the residual velocity increases almost linearly except at the impact velocities very close to the ballistic limit velocity. The relationships between impact velocity and residual velocity for room temperature (R.T.) and 1000 °C make little difference in the case of SiC and ZrO<sub>2</sub> and they are almost identical. However, for a higher temperature of 1350 °C, the residual velocities for SiC are higher than those of R.T. and 1000 °C for the same impact velocities, while those for ZrO<sub>2</sub> are reversed. This means that the ballistic impact property of ZrO<sub>2</sub> improves at an elevated temperature of 1350 °C. The ballistic limit velocities  $V_b$  are estimated from Eq.(1) along with Eq. (3), which, in the case of R.T. and 1000 °C, are 99.2 m/s and 85.0 m/s for SiC and ZrO<sub>2</sub>, respectively. Substituting these ballistic limit velocities into

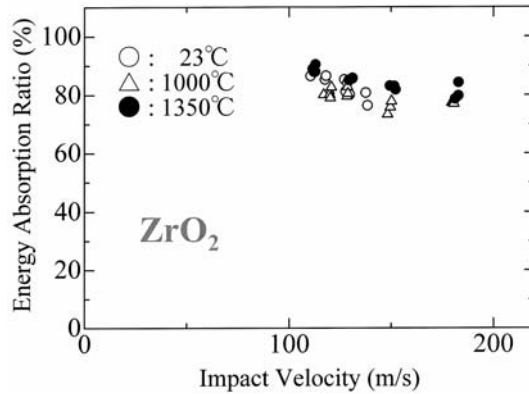
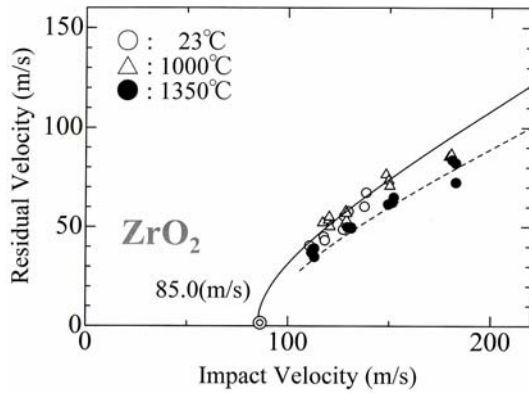
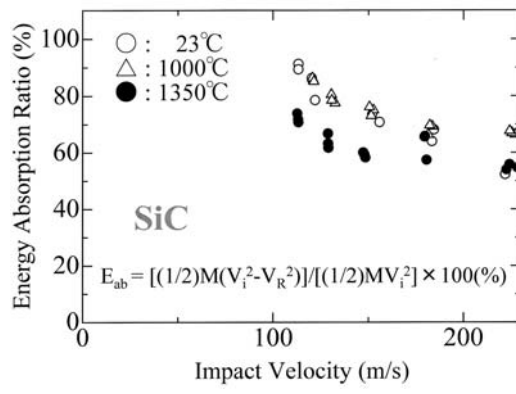
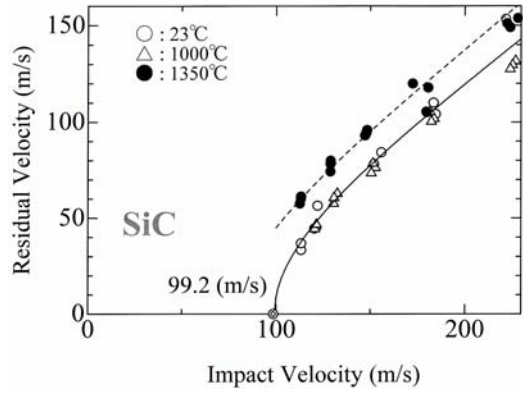


Figure 8: Residual velocity

Figure 9: Energy absorption ratio

Eq. (2), we have the predicted residual velocities, which are represented by solid lines in both figures. The corresponding results for  $\text{Al}_2\text{O}_3$  and  $\text{Si}_3\text{N}_4$  are found to be similar to those of  $\text{SiC}$ . The ballistic limit velocities for  $\text{Al}_2\text{O}_3$  and  $\text{Si}_3\text{N}_4$  are 96.6 m/s and 104.3 m/s, respectively.

Figure 9 shows the energy absorption ratio  $E_{ab}$  for  $\text{SiC}$  and  $\text{ZrO}_2$  that is defined by the ratio of the difference of the kinetic energies of the projectile before and after impact perforation to the initial kinetic energy (before impact). It decreases with an increasing impact velocity and the decreasing rate is higher for  $\text{SiC}$  than for  $\text{ZrO}_2$ . The ratio for  $\text{SiC}$  is lower for 1350 °C than for R.T. and 1000 °C, while the situation is reversed for  $\text{ZrO}_2$ . The corresponding energy absorption ratios as a function of impact velocity for  $\text{Al}_2\text{O}_3$  and  $\text{Si}_3\text{N}_4$  are found to be almost the same as that of  $\text{SiC}$ .

Figure 10 shows the residual velocity and energy absorption ratio as a function of impact velocity for a temperature of 1350 °C, in which the results for the four kinds of

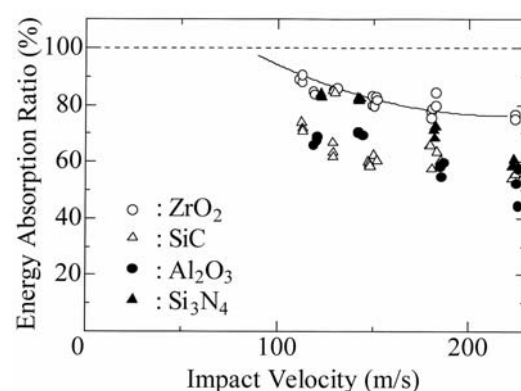
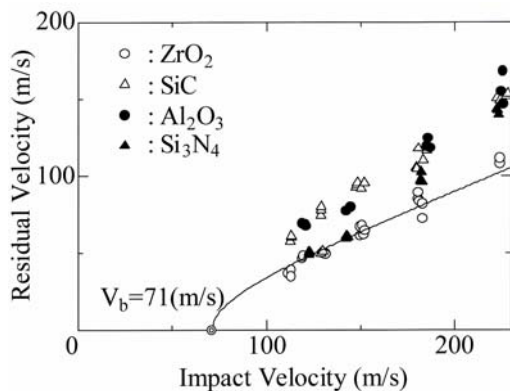


Figure 10: Residual velocity (left) and energy absorption ratio (right) for 1350 °C

ceramic materials tested in the present study are collected. It is found that, in general, the residual velocity for ZrO<sub>2</sub> is lower than those of Al<sub>2</sub>O<sub>3</sub>, Si<sub>3</sub>N<sub>4</sub>, and SiC, while its energy absorption ratio is higher than those of the others. This means that the ballistic impact property of ZrO<sub>2</sub> is superior to Al<sub>2</sub>O<sub>3</sub>, Si<sub>3</sub>N<sub>4</sub>, and SiC at a high temperature of 1350 °C. The ballistic limit velocity for ZrO<sub>2</sub> is estimated to be 71 m/s.

## 6. CONCLUSIONS

In order to evaluate the ballistic impact properties of monolithic ceramic materials at high temperatures, a high-temperature impact test system is developed by incorporating a high temperature furnace and a digital imaging system into a gas gun type impact machine. This system facilitates the visualization of the impact behavior of the target materials at high temperatures as well as at room temperature. The effect of high temperatures on the ballistic impact properties of these ceramic materials is found to be more remarkable at a high temperature of 1350 °C rather than at room temperature and 1000 °C. We also find that the ballistic impact properties of ZrO<sub>2</sub> are very different from those of other ceramics Al<sub>2</sub>O<sub>3</sub>, Si<sub>3</sub>N<sub>4</sub>, and SiC. From the present study, the ballistic impact properties of these ceramic materials at high temperatures are examined successfully.

## ACKNOWLEDGEMENTS

The work presented here has been funded by the Ministry of Education in the project to build centers for high-tech research in private universities. Their support is gratefully acknowledged. The authors also express their sincere appreciation to the many contributions of their students in the mechanics of materials laboratory at Takushoku University.

## REFERENCES

- 1- Wimmer, J.M. and Bransky, I. 1977. "Impact Resistance of Structural Ceramics", *American Ceramic Society Bulletin*, 1977; 56:6:552-560.
- 2- Liaw, B.M. Kobayashi, A.S. and Emery, A.F.. "Theoretical Model of Impact Damage in Structural Ceramics", *Journal of American Ceramic Society*, 1984; 67:8:544-548.
- 3- Hsueh, C.H. and Hui, D., "Foreword", *Composites Engineering*, 1995; 5:10: VII-IX.
- 4- Ishikawa, T. et al., "A Tough, Thermally Conductive Silicon Carbide Composite with High Strength up to 1600°C in Air", *Science*, 1998; 282:1295-1297.
- 5- Report on 300kW Class Ceramic Gas Turbine, NEDO and CGT R&D Association .1999.
- 6- Kasano, H., "Impact Perforation of Orthotropic and Quasi-isotropic CFRP Laminates by A Steel Ball Projectile", *Advanced Composite Materials*, 2001; 10:4:309-318.
- 7- Kasano, H. and Hasegawa, O., "Ballistic Impact Behavior and Properties of Structural Ceramic Materials", *Proc. 7<sup>th</sup> Japan Int. SAMPE*, 2001; 891-894.
- 8- Kasano, H. and Hasegawa, O., "Ballistic Impact Properties and Behavior of Structural Ceramics at High Temperature", *Proc. 10<sup>th</sup> U.S.-Japan Conf. Composite Materials*, 2002; 581-587.